



A survey on the gas emissions and soil properties near the surface in a coal fire area

Haiyan Wang¹ · Junpeng Zhang¹ · Lei Zhang¹ · Jiali Wang¹ · Zuohui Xu¹

Received: 27 July 2020 / Accepted: 16 February 2021 / Published online: 26 February 2021
© Saudi Society for Geosciences 2021

Abstract

In this study, a comprehensive survey was performed on the fire-induced landforms, belowground and near surface gas emissions, and soil properties. In addition, the effect of the soil cover on the gas emissions and soil properties was examined. The survey zone was divided into three areas based on the surface features. Sponges, vents and cracks, and the fissures dominated in area A, and area B exhibited no obvious features but was covered with a layer of sand soil. Area C was characterized by degraded vegetation. A comparison of the composition and concentration of belowground and near surface gases was performed among the three areas. Topsoil samples were collected at a 0–5-cm depth in the three areas, and soil properties were measured and analyzed. The average CO, CO₂, CH₄, and H₂ concentrations below the ground surface in area B were lower than those in area A. The detected near surface CO and CH₄ mainly originated from obvious openings. Damage to the soil ecology was primarily caused by the replacement of O₂ by CO₂. Soil thermal and humidity anomalies were obvious in area A, but scarcely occurred in areas B and C because of solar heating. The soil pH was the lowest in area A, which was closely related to the total soil contents. The organic matter contents in area B were higher than those in area A because of the increase in the particles released from underground coal fires, and area C attained the highest organic matter contents due to vegetation withering.

Keyword Coal fires · Emitted gases · Soil properties · Soil cover

Introduction

Underground coal fires are natural hazards which the coal experiences oxidation, thermal accumulation, and eventually spontaneous ignition (Liang et al. 2016), generally occurring in exposed coal seams, coal storage piles, or coal waste piles (Jiang et al. 2017). Coal fires consume non-renewable coal resources and release tremendous amount of toxic gases (e.g., CO and SO₂), greenhouse gases (e.g., CO₂ and CH₄), and trace elements (e.g., As, F, and Hg). In addition, underground coal fires contribute to land subsidence due to volume loss of coal seams (Kuenzer and Stracher 2012), and threaten the lives and properties of local residents. To date, research on underground coal fires in the environment has focused on the

assessment of soil gas emissions, underground water, and soil pollution (Song and Kuenzer 2014).

Pone et al. collected and analyzed gas combustion by-products from gas vents in the Witbank and Sasolburg coal-fields, and assessed the health risk to local communities (Pone et al. 2007). Carras et al. measured greenhouse gas emissions originating from spoil piles and waste coal dumps, and studied the difference in gas emissions among three areas characterized by the extent of spontaneous combustion (Carras et al. 2009). Temporal and spatial gas (e.g., CO₂, CO, Hg, and hazardous pollutants) trends of vent dynamics were extensively investigated (Dindarloo et al. 2015; Engle et al. 2012; Garrison et al. 2017; Hower et al. 2009, 2011, 2013; O'Keefe et al. 2010, 2011). Gaseous emissions may condense in the mouth of gas vents due to the sharp decrease in temperature, and the characteristics of the secondary minerals of the condensates have been investigated, including the components and the formation mechanisms (Dias et al. 2014; O'Keefe et al. 2018; Oliveira et al. 2019). Some gaseous emissions are highly soluble, and liquor leaching may lead to severe acid drainage, resulting in pollution of underground water (Querol et al. 2011). In addition, the toxic trace elements

Responsible Editor: Amjad Kallel

✉ Junpeng Zhang
sdbzjp@126.com

¹ School of Emergency Management and Safety Engineering, China University of Mining & Technology, Beijing 100083, Beijing, China

(e.g., As, F, Hg, and Se) emitted by the underground coal fires may become enriched in gas vents and soils (Hong et al. 2018; Liang et al. 2018; Li et al. 2018), thus causing soil contamination. Changes in soil properties could also influence the distribution of soil heavy metals and polycyclic aromatic hydrocarbons (PAHs) in coalfields, which in turn could aggravate the destruction of terrestrial ecosystems. Querol et al. found that mobility of certain trace pollutants was enhanced under acidic conditions, such as Li, Ti, Sc, V, Cr, Mn, Co, and Ni. In addition, Al-K-Fe-NH⁴⁺-bearing sulfates easily dissolved under acidic conditions (Querol et al. 2008). Garrison et al. observed that the concentrations of monoaromatic hydrocarbons (BTEX) and PAHs in soils were higher in areas with high soil matter contents due to their enhanced absorption capacities (Garrison et al. 2016). Wang et al. observed that soil Hg and Cd exhibited notable correlations with total carbon contents, and suggested that soil Hg and Cd were related to organic matter (Wang et al. 2019). Therefore, the study of soil properties contributes to explaining the formation and distribution of certain soil pollutants.

A small, but growing, body of research has been conducted to investigate the impact of underground coal fires on the soil properties in coal fire areas. Tobin-Janzen et al. found changes in resident microbial populations in boreholes impacted by Centralia, and Pennsylvania anthracite coal fires, and the soil temperature, pH, and chemical composition were analyzed (Tobin-Janzen et al. 2005). Zhang et al. performed physicochemical characterization of soil samples in the mouths of vents, and microbial communities at high temperatures (Zhang et al. 2013). Zeng et al. investigated surface vegetation coverage, heavy metal distribution, and organic matter, and determined that coal fires can affect soil properties via organic matter digestion (Zeng et al. 2018). However, most of the research on soil properties has focused on vents or surface openings, in addition to the soil gas emissions.

The aims of this investigation are to (1) analyze the concentrations of hazardous pollutants in various soil layers in Wuhushan coal fires not confined to vents or surface openings and (2) collect and analyze surface soil samples to conduct the soil physicochemical characterization in the investigated area. In addition, the effect of backfill consisting of sandy soils on the gas emissions and soil properties is examined.

Materials and methods

Site description

The Wuda coalfield is located in the northwest of Wuda District, and including three coal mines: Wuhushan, Suhaitu, and Huangbaici (Fig. 1), covering an area of 35 km². The study area is a backfilled region in the northern Wuhushan mine, which belongs to the no. 10 fire zone. The climate in

the area is characterized as a strongly continental, semiarid climate, with an average precipitation of approximately 168 mm/a (Song and Kuenzer 2017). The land surface of the Wuhushan coalfield is dominated by bare rocks covering sandy soil, and the vegetation density is very low (Song et al. 2015). The Wuhushan coal mine started construction in 1965. The no. 9, no. 10, no. 12, no. 13, no. 15, no. 16, and no. 17 coal seams are the main coal seams in the Wuhushan mine, among which the no. 9, no. 10, and no. 12 exhibit a high propensity of spontaneous combustion with sulfur contents up to 3.42%. Notably, in-ground coal fires occur when shallow coal seams are exposed at the Earth's surface (Shan et al. 2019). The destructive and disorderly operation of small-scale private mine results in the spread of coal fires. Since 2006, a coal fire suppression project has been implemented in the area. Coal mines are typically contracted to individuals, and they are permitted to excavate surface rocks, remove spontaneous combustion coal, and sold any mineable coal, but they are responsible for backfilling. However, exaction has destroyed the landscape, and new fissures and cracks have thus been created, which has led to the expansion of the coal fire range. The above scheme has been terminated by the local government, and a fire suppression project was gradually implemented towards standardization in 2011. Follow-up work was organized and implemented by a professional fire-fighting engineering office (Liang 2018). The burning coal was excavated, the ground surface was covered with sandy soil, and sowing grass were sown for ecological restoration purposes. This method obtained promising results, and the area of shallow and visible coal fires was estimated to have decreased by ~60%, while the risk of spreading remains (Jiang et al. 2017). In the research zone, the intensity of shallow coal fires notably decreased, and recovery of vegetation was observed along the edge of the survey zone. However, the overlying soil did not prevent hidden combustion of coal seams. Nearly all the surfaces were devoid of vegetation in the high-temperature zone. Visible surface flames were extinguished, but fumes persisted scattered throughout the central area.

Gas concentrations were measured on a variety of surfaces grouped into three categories based on the degree of combustion of the underground coal fire:

- 1) Surfaces with spontaneous combustion and obvious features, including cracks (Fig. 3b), sponges (Fig. 3c), fissures (Fig. 3d), and vents (Fig. 3e). This region was defined as area A.
- 2) Surface with spontaneous combustion but without any obvious features covered by sandy soils. This region is defined as area B.
- 3) Surfaces characterized by withered plants (Fig. 3e). The vegetation degradation area occurred along the periphery of the investigated area (Fig. 2). It represented the

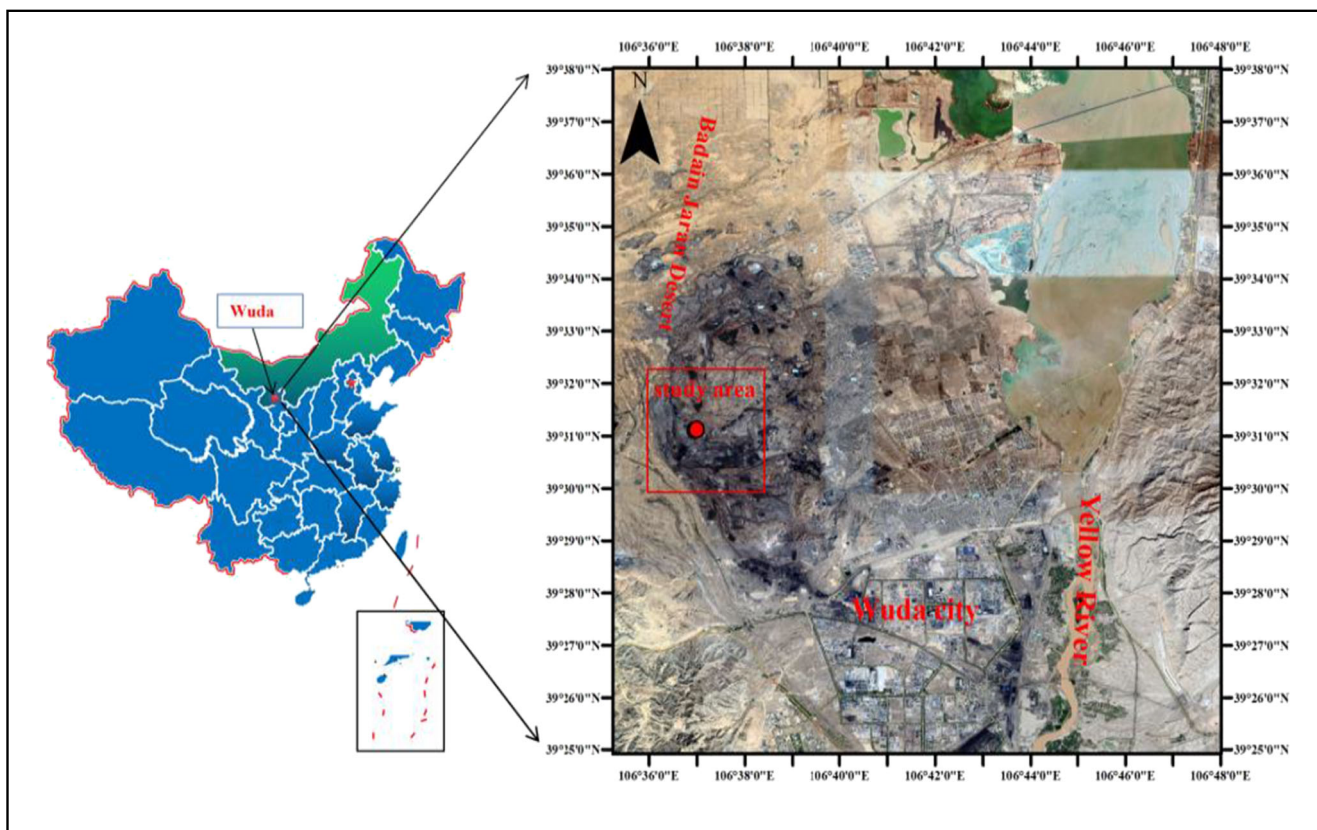


Fig. 1 Location of the coal fire in the Wuda Coalfield, Inner Mongolia, China (The source of the figure is from the Google maps)

reclamation area, in which coal fires had been extinguished, and grass seeds were sown for ecological restoration. This region was defined as area C.

The coal fire-induced landforms can be roughly divided into three types among the backfilled regions in area A, including cracks and vents, sponges, and fissures. Cracks and vents are distributed in the southeastern sampling areas, and obvious black smoke is observed. The maximum width of the cracks is approximately 70cm, and they are possible pathways for the ventilation of the underground coal fires (Kuenzer and Stracher 2012). Compared to the original landform (Engle et al. 2012), the observed vents and cracks contained no visible minerals or tars (Fig. 3b). The soil cover may contribute to the lack of tar and minerals. The fissures are mainly distributed in the northwestern part of the investigated area. The fissures are linear in the surface soil, and they are common out-bound pathways of hot gas emissions (Kuenzer and Stracher 2012). The in situ fissures range from a few centimeters, and are extremely narrow (<0.5 cm), and white and yellow salt minerals could be observed besides the fissures. When hot particulate emissions cool, the substances absorb water and change into white salts which mainly consist of alunogen (Querol et al. 2011). The yellow salts mainly comprise native sulfur, which is generated the reaction: $\text{SO}_2 + 2\text{H}_2\text{S} \rightarrow 3\text{S}_0 +$

$2\text{H}_2\text{O}$ (Querol et al. 2008). The presence of the sulfur also suggests that the coal fire is located deep below the ground surface, because sulfur only remains stable below 100°C (Gürdal et al. 2015), which is also confirmed by measurement of the temperature in situ (Fig. 4). Sponges are a type of sponge-like contaminated soil (Liang et al. 2018), commonly found on the surface of the backfilled regions, and are mainly distributed in the southeast, as shown in Fig. 3e.

Soil sampling

A soil and gas sampling campaign was carried out in August, 2019. A total of 88 soil samples at depths ranging from 0 to 5 cm was collected with a Teflon tool at closely spaced intervals (10m), of which 30 samples were collected in area A, 46 samples were collected in area B, and the remaining samples were collected in area C.

Surface gas concentration measurements

H_2S , SO_2 , and H_2 were measured in situ, and monitoring was performed with a portable gas analyzer containing a self-priming pump. The range and accuracy of the emission analyzer are 0–2000 ppm and $\pm 0.1\%$, respectively, for H_2 and 0–100 ppm and $\pm 1\%$, respectively, for SO_2 and H_2S . The probe of the sampling device was hammed to a depth of

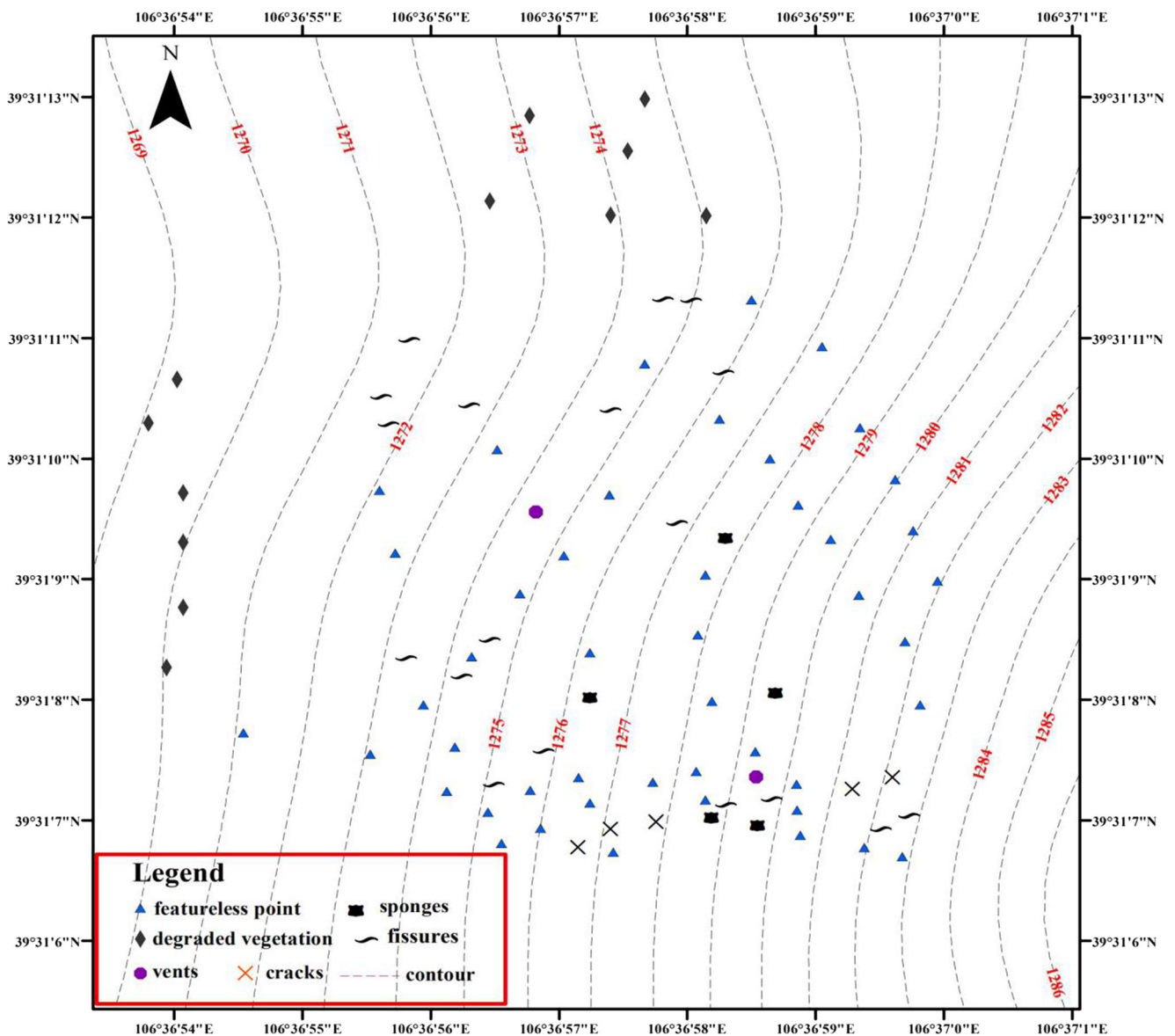


Fig. 2 The sampling location

approximately 5 cm at each grid point, and connected to the gas inlet of the analyzer. In area A, a rubber tube was directly inserted into the vents and cracks. Measurement was recorded until the date remained stable during the process of measurement. CO, CO₂, CH₄, C₂H₆, C₂H₄, C₂H₂, N₂, and O₂ were analyzed via capillary gas chromatography (GC-4000A, Beijing), and the accuracy assessed via standard gas mixture was less than 5%, while the reproducibility was higher than 10%. Belowground gases were drawn with a gas-tight syringe, and injected into cleaned aluminum foil sampling bags. Moreover, near-surface gases were directly drawn with a gas-tight syringe at a vertical distance of 70 cm from the position corresponding to the belowground gases. The airbags were transferred to the laboratory within 24 h.

Soil chemical analyses

The soil pH was determined with various pH meters, and the organic matter content was measured via potassium dichromate oxidation. The soil humidity was measured with a portable digital hygrometer. The total salt contents were determined via measurement of the electrical conductivity of the soil leaching solution. The distribution of the soil pH and total salt contents in the investigated area were interpolated via the inverse distance weighting method in ArcGIS 10.4, as shown in Fig. 6.

Surface temperature measurement

The surface temperature was measured with an infrared thermal imager (Fortric220s, USA), and the measurement range

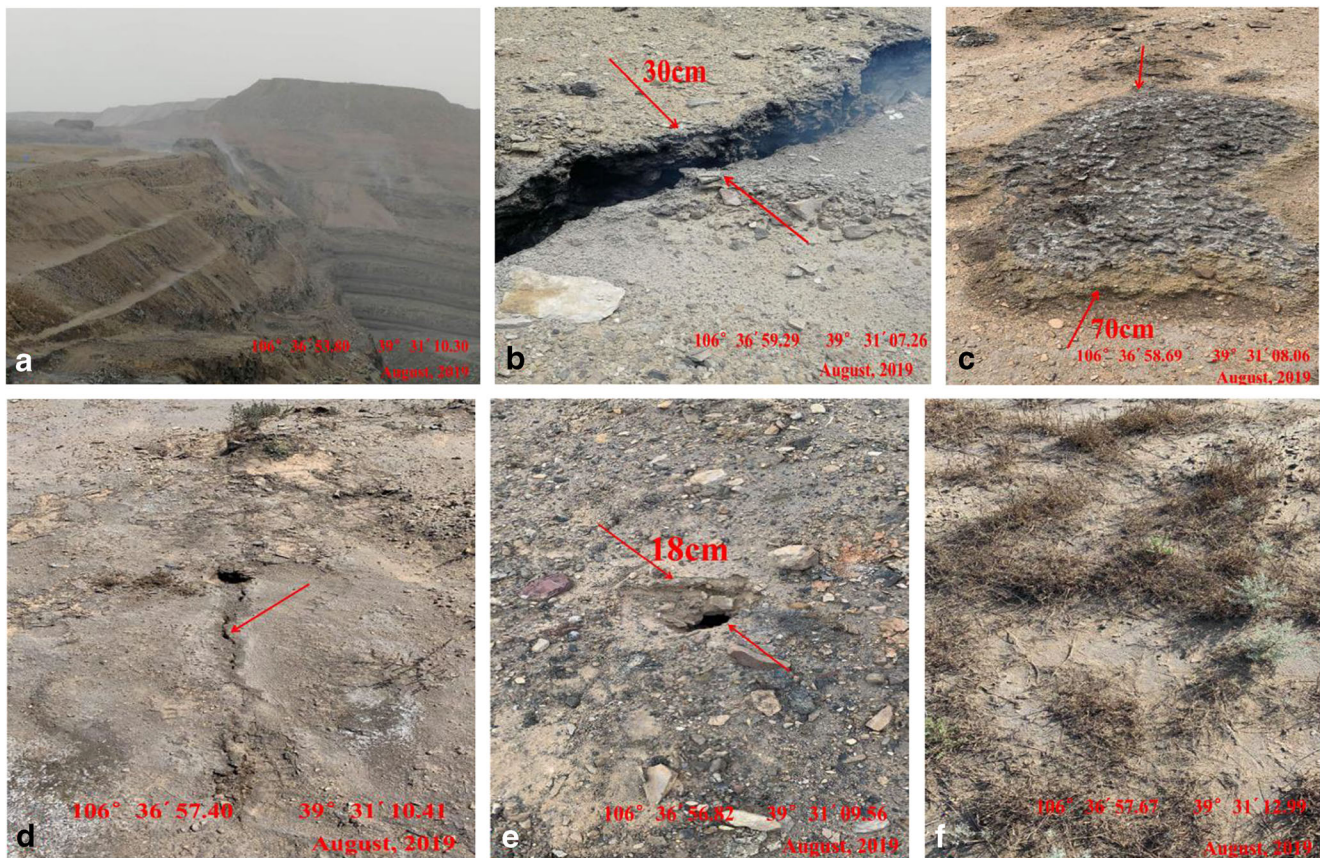


Fig. 3 Landscapes of the research zone. **b** Crack. **c** Sponge. **d** Fissure. **e** Vent. **f** Degraded vegetation

and accuracy of the imager are -20 to 150 °C and ± 0.1 °C, respectively. The highest temperature in the images (e.g., the vent in Fig. 3) was selected as the representative temperature. The surface temperature and soil moisture were also interpolated via the inverse distance weighting method in ArcGIS 10.4, as shown in Fig. 3.

Statistical analysis

A statistical *t* test was performed to statistically determine whether the soil properties in the different areas, including the soil organic matter content, soil pH, and total salt contents, were significantly different ($p \leq 0.01$).

Results and discussion

Analysis of the soil physical properties

The ground temperature in area A is significantly higher than that in area B (Fig. 3b), which indicates that the temperature is mainly transmitted to the surface via convection through the cracks and fractures. The variation in the ground temperature is high among the various fire-induced landforms. The maximum temperature in the cracks reaches 354 °C (Table 4), significantly

higher than that at the sampling points, which indicates that the fire front may lie in the southeastern part of the investigated area.

The cracks are linearly oriented from SW to NE, and it is inferred that the underground coal fires move from SE to NW based on the cracks that are orthogonal to the fire spreading direction. The average surface temperature of the sponges is the highest, and the sandy soil is very dark gray because of combustion and particle emission. The surface temperature of the fissures ranges from the 36.4 to 261 °C (Table 4), and the average temperature is the lowest among all the points with obvious features (Table 4).

The soil humidity is correlated with the combustion degree of the underground coal fire. The contours of the soil humidity are dense in areas where the combustion degree is high (Fig. 3). The soil near the sponges obtained the highest water contents, followed by the fissures (Table 4). Humid soil is almost undetectable in the degraded area due to the influence of solar radiation. In area B, at 25% of the points, humid soil is detected, mostly ranging from 2.1 to 10.1% (Table 4), and humid soil mainly occurs at the center of the high-temperature zone (Fig. 3). Research has shown the coal may contain more than 20% moisture by weight (Gürdal et al. 2015), and the vapor may seep to the surface along fissures within the bedrock by the buoyancy generated via heating, and it may accumulate in soil near the fissures and vents, thus increasing the soil

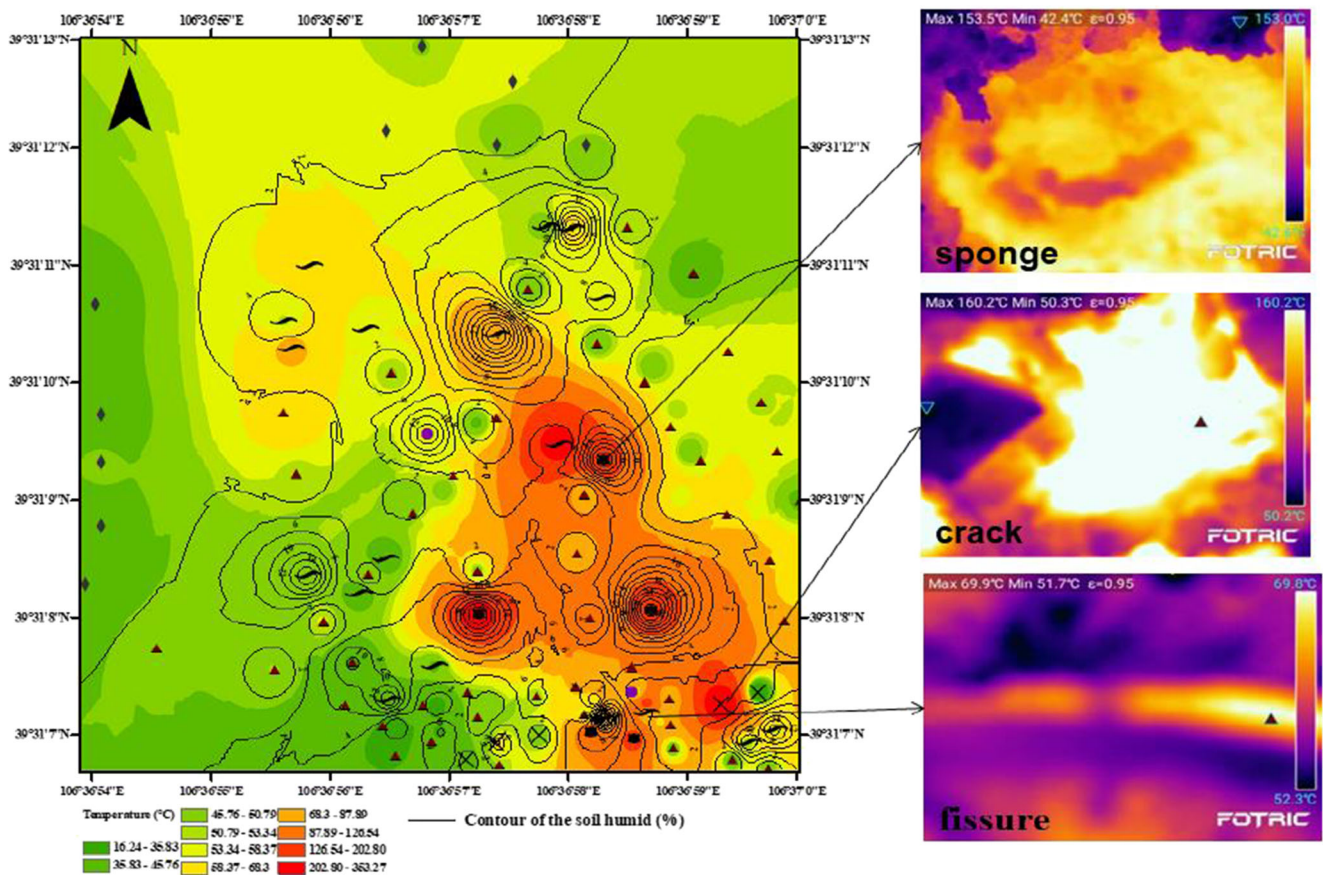


Fig. 4 The distribution of surface temperature and soil humid in the research zone

humidity. The average soil humidity near fissures and sponges is higher than that near the vents and cracks (Fig. 3), because the former are more likely to act as outbound ventilation pathways (Kuenzer and Stracher 2012).

Analysis of the belowground gas concentration

Coal fire gases are transported to the surface through two primary mechanisms: advection through vents and fractures (vent emissions) and diffusion through the overburden (O'keefe et al. 2018). Gases are released in area A via advection, while diffusion dominates in area B. CO_2 , CO, and CH_4 are the dominant gases in the research zone with additional components such as H_2 , SO_2 , H_2S , C_2H_4 , C_2H_2 , and C_2H_6 . These gaseous products may be largely generated via the thermal degradation of the biopolymers occurring in coal seams. The CO_2 concentrations are relatively high in the vicinity of the fire front (Fig. 6), with the highest CO_2 concentration reaching 11 vol%. The concentrations of CO_2 seem to exhibit no correlation with the surface temperature, which is contrary to the conclusions of Hower et al. (2009). This probably occurs because gas emissions are more likely dominated by the underground fire itself, not the surface temperature. In addition, the distance to the fire or the presence of obstacles also influences the ground temperature and gas

emissions (Garrison et al. 2017). The variation in the belowground CO_2 concentration in area A is wide (Table 1), and is influenced by the fire depth, ventilation area, and relative position of the fire front to the vent (O'keefe et al. 2011; Song et al. 2019, 2020). The average CO_2 concentration in area A is 5.4 vol% (Table 1), significantly exceeding the OSHA 8-h limit of 5 vol%. In the area B, the average CO_2 concentration is of the same order of magnitude as that in area A (Table 2), which indicates a relatively high permeability, of the thin calcite-cemented sandstone occurring below surface soil layer. The variation differs within a range of 3 orders of magnitude in area B (Table 2), and there are two main reasons for the high variation. On the one hand, cracks, vents, and fissures are established before landfilling, but may remain still active despite the sandy soil cover. On the other hand, dense fissures and tectonic discontinuities occur within various strata of the formations.

The vegetation cover is low in the investigated area (Fig. 4f), of which areas A and B are covered with little or no vegetation. Kuenzer et al. found that toxic gases and underground heat are responsible for the deterioration of vegetation (Kuenzer et al. 2007). A strongly negative relationship is found between the soil CO_2 and O_2 concentrations in areas A and B (Fig. 5), which indicates that the soil O_2 is displaced by CO_2 produced by the underground coal fire. Patil et al. suggested that a minimum soil

Table 1 Principal statistical parameters of multiple gases in area A

	CO ₂	Ground CO ₂	CO	Ground CO	CH ₄	Ground CH ₄	C ₂ H ₄	C ₂ H ₆	H ₂	SO ₂	H ₂ S	O ₂	N ₂
Percentage of samples (%)	100	100	100	100	100	100	76.5	23.3	96	100	76.5	100	100
Mean (ppm)	54,067	1854	696	22	646	38	23	37	401	6.39	16	64,044	740,524
Standard deviation	31,500	948	1238	15	508	149	25	42	412	5.8	25	14,309	21,433
Minimum	1647	18	9	9	4	2	2	6	17	0.73	2	32,324	697,750
Maximum	110,000	3824	6008	68	2274	823	74	128	1200	26.40	100	90,394	818,313

O₂ concentration ranging 12–14% could sustain a healthy root environment, or the plant would wither due to a decreased root respiration (Patil et al. 2010). However, the maximum O₂ concentration in the degraded area the least affected by underground coal fires is lower than 10 vol% (Table 3). Therefore, anoxic conditions are also a major factor causing ecological environmental damage.

Compared to the vents and cracks in the Heshituoluogai coal fire area (Wang et al. 2017), H₂ is detected at most points in area A, and the average H₂ concentration is 401 ppm (Table 1), which is significantly higher than that in the Heshituoluogai coal fire area. The high concentration of H₂ indicates that the underground coal fire occurs in the advanced heating phase. The CO and CH₄ concentrations in area A are lower than the CO₂ concentration, indicating that the system is approaching near-complete combustion conditions. CO, ranging from 9 to 6008 ppm (Table 1), far exceeds the 8-h OSHA limit of 50 ppm. The CH₄ concentration ranges from 4 to 2274 ppm (Table 1). In comparison to Tiptop coal-mine (O'keefe et al. 2018), the high CH₄ concentration also indicates that the coal fire occurs in the stage of intense combustion. The CO and CH₄ concentrations in the area B are significantly lower than those in area A, while the range of the concentrations is large, ranging from 4 to 3530.3 ppm and 1 to 2276 ppm (Table 2), respectively. C₂H₄ is detected in almost 76.5% of the analyzed samples in area A, and its concentrations reach up to 74 ppm (Table 1). Compared to C₂H₄, C₂H₆ is detected in almost 23.3% of the analyzed samples, and C₂H₄ and C₂H₆ are detected only in trace amounts: in fewer than 39% and 7%, respectively, of the analyzed samples (Table 1). H₂S and SO₂ are highly concentrated in

area A, ranging from 0.72 to 26.4, and 2 to 100, respectively (Table 1).

In the degraded vegetation area, H₂, SO₂, and H₂S are not detected. The belowground CO and CH₄ concentrations are low, averaging approximately 7.11 ppm and 10.9 ppm, respectively (Table 3). A moderately negative relationship is found between the soil CO₂ and CH₄ concentrations in area A ($r=0.727$, $p<0.01$, $n=30$), indicating that they have the same origin, and most of the gases may be generated from the combustion of coal. The CO concentration does not seem related to the CO₂ concentration in areas A and B. This indicates that the system occurs in an unsteady state, and CO may be rapidly converted into CO₂. Although landfills may prevent the emission of CO, SO₂, H₂S, C₂H₂, C₂H₄, and C₂H₆, the average CO₂ and CH₄ concentrations are the same order of magnitude in areas A and B (Table 3). This indicates that the degree of greenhouse gas emissions through soil diffusion in the backfilling area also contributes to the burden of the atmosphere. Therefore, the estimation of greenhouse gas emission through soil diffusion in backfilling areas deserves attention.

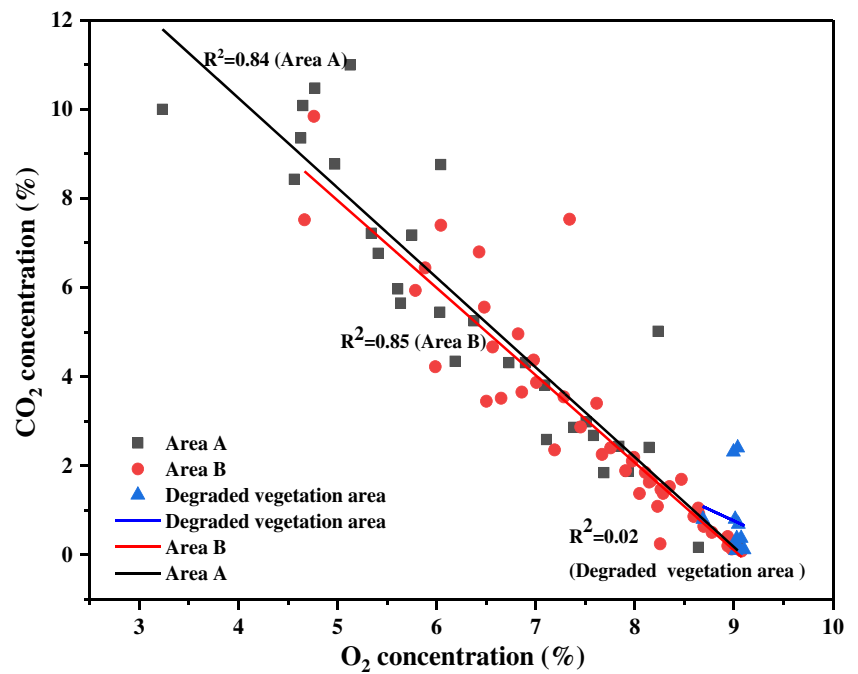
Analysis of the near-surface gas concentration

The near-surface CO₂ concentration is relatively high in area A, and the maximum value is below the OSHA 8-h limit of 0.5 vol% (Table 1). The contours of the near-surface CO₂ concentration are dense in the vicinity of the high-temperature zones, but sparse in the area far from the high-temperature zones (Fig. 6). The average concentration of CO₂ is 839 ppm in the vicinity of the degraded vegetation area (Table 3), almost unaffected by underground coal fires. Near-surface CH₄ and

Table 2 Principal statistical parameters of multiple gases in the area B

	CO ₂	Ground CO ₂	CO	Ground CO	CH ₄	Ground CH ₄	C ₂ H ₄	C ₂ H ₆	H ₂	SO ₂	H ₂ S	O ₂	N ₂
Percentage of samples (%)	100	100	100	100	100	100	39	7	70.4	48.4	27.8	100	100
Mean (ppm)	28,662	1161	281	16.6	286	118	25	69	304	2.86	14.4	76,000	732,425
Standard deviation	24,191	573	649	8.8	480	324	24	84	394	2.7	14.6	11,359	12,199
Minimum	838	677	4	10.0	1	3	3	16	2	0.54	1	46,658	697,639
Maximum	98,456	4120	3530	46.42	2276	1243	89	166	1100	8.00	47	90,782	760,280

Fig. 5 Correlation between soil CO₂ and O₂ concentrations in the investigated area



CO are also detected in area A, but their concentrations are lower than their corresponding belowground concentrations (Table 1). The maximum ground concentration of CO is 68 ppm in area A (Table 1), which is slightly higher than the eight-hour OSHA limit of 50 ppm. Obviously, gases are diluted by air as they are emitted, but temperature inversions can cause potential health risks in the surrounding regions of coal fire areas (Hower et al. 2009). The correlation of the belowground CO₂ concentration with near-surface CO₂ concentration in area A is positive but not significant ($R^2=0.38$, $p<0.01$, $n=30$), and in area B, there seems to be no association ($R^2=0.17$, $P=0.01$, $n=58$). This suggests that gases generated from the vents, cracks, and fissures mainly affect the near-surface CO₂ concentration distribution. The near-surface CO and CH₄ concentrations in area B are in line with these same rules. The near-surface CH₄ concentrations at same locations are even higher than their corresponding belowground CH₄ concentrations due to the influence of vent advection. H₂, SO₂, H₂S, C₂H₄, C₂H₆, and C₂H₂ are below the detection limits in the near-surface zone (Table 2).

Analysis of the soil total salt contents and soil pH

Area A exhibits the lowest soil pH, with an average value of 5.35, and it mostly ranges from 4.03 to 6.67 (Table 4). Several studies of the soil pH distribution impacted by underground coal fires can be referenced for comparison. Tobin-Janzen et al. found that the soil pH in surface soil samples (at a depth from 0 to 20 cm) collected in boreholes indicated slightly acidic to acidic conditions throughout the Pennsylvania mine fire area (6.35–4.11) (Tobin-Janzen et al. 2005). Wang et al. measured the soil properties around the vents, and found that the soil pH and total salt contents near vents varied although they originated from same coal seam, and the data indicated that the soil pH was correlated with the total salt contents (Wang et al. 2020). The soil pH observed in this study is not consistent with the above reports because of the difference in the environment among the areas. However, these studies all indicate that the soil pH near the vents and cracks is generally acidic.

Table 3 Principal statistical parameters of multiple gases in the degraded vegetation area

	CO ₂	Ground CO ₂	CO	Ground CO	CH ₄	Ground CH ₄	C ₂ H ₄	C ₂ H ₆	H ₂	SO ₂	H ₂ S	O ₂	N ₂
Percentage of samples	100	100	100	100	100	100	-	-	-	-	-	100	100
Mean (ppm)	7298	839	10	11	7	3.18	-	-	-	-	-	84,491	729,726
Standard deviation	7990	138	3	1	5	0.48	-	-	-	-	-	10,261	27,394
Minimum	970	613	6	10	2	2.6	-	-	-	-	-	53,723	694,615
Maximum	24,012	1017	15	12	19	4.02	-	-	-	-	-	90,667	806,999

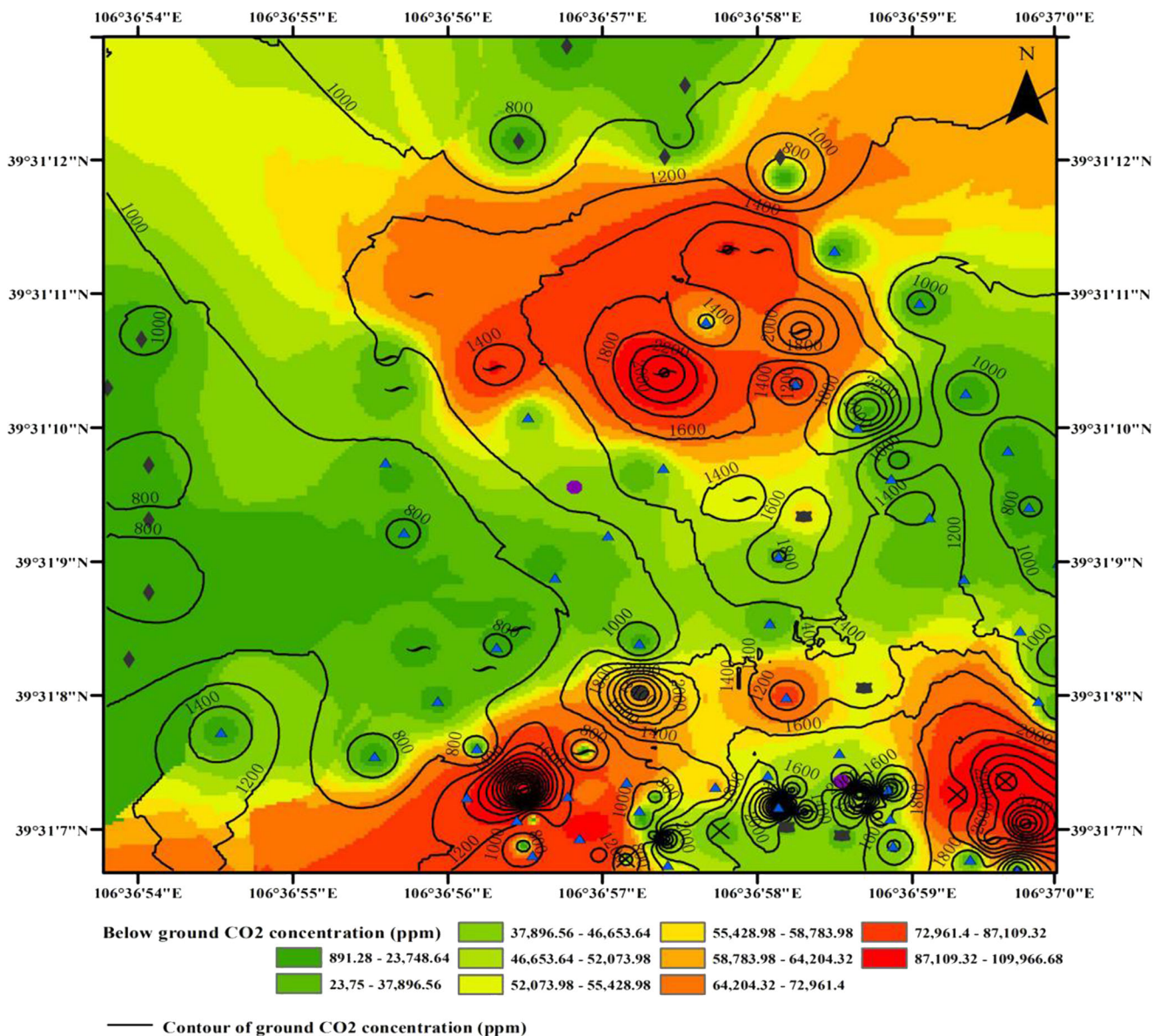


Fig. 6 The distribution of CO₂ concentration in the investigation area

The average soil pH varied greatly among the landforms in area A, and the sponges in the area exhibited the lowest soil pH (0.95–1.99), followed by the vents and cracks (1.57–7.18), while the soil pH near the fissures was the highest (3.09–7.79) (Table 4). The negative correlation between the soil pH and the total salt contents ($r=0.859, p<0.01$) indicated that the soil pH is significantly influenced by the soil salt in area A (Fig. 7). A source for a high acidity may be hydrolysis of the sulfate, while $Fe^{3+}-Fe(OH)^{2+}$ and $HSO_4^{-}-SO_4^{2-}$ could maintain a pH of approximately 1, while the dissolution of alunogen and the hydrolysis of other Al sulfates may be responsible for a pH values of approximately 4 (Querol et al. 2011). Most samples retrieved from the fissures indicated near-neutral pH, and the significant leachable content of gypsum (high Ca and SO_4^{2-}) may be unaffected by pH. A

small number of samples collected from the fissures even indicated alkalinity, and NH_4Cl and organic condensates could account for this alkalinity (Querol et al. 2011). Sulfate in area A could be generated by the reaction of SO_2 with the soil moisture, which is confirmed by the high SO_2 concentration in the area (Fig. 7). The average soil pH was 7.19 in area B, and significantly lower than that in area A (Fig. 8). This indicates that the soil cover weakens the acidity, which plays a positive role in reducing environmental hazards. Compared to area A, the total salt contents were significantly lower than those in area B (Fig. 8), and the contours of the SO_2 concentration were relatively sparse (Fig. 7). SO_2 was even not detected in the degraded vegetation area (Fig. 7). The soil pH in area B was relatively higher than that in area C (Fig. 8), but

Table 4 The soil properties in the area A

Categories		Surface temperature (°C)	The soil humid (%)	Soil total salt contents (dS/m)	Soil pH	Soil organic carbon contents (mg/g)
Fissures	Number of measurements	<i>n</i> =18				
	Minimum	36.4	2	1.41	3.09	2.80
	Maximum	261	26	9.42	7.79	21.41
	Mean	67.6	9.69	4.22	6.74	13.41
	Standard deviation	49.9	7.93	2.13	1.25	5.50
Sponges	Number of measurements	<i>n</i> =5				
	Minimum	126	5	13.25	0.95	9.41
	Maximum	277	27.2	20	1.99	17.65
	Mean	174.9	16.72	18.65	1.43	11.88
	Standard deviation	58.7	9.35	3.02	0.51	3.41
Cracks and vents	Number of measurements	<i>n</i> =7				
	Minimum	44	3.5	1.28	1.57	7.26
	Maximum	354	6.02	16.66	7.18	13.51
	Mean	152	0	5.35	4.56	10.48
	Standard deviation	139	13	5.29	2.05	2.5

the *t* test showed that there was no significant difference between these two groups.

Analysis of the organic matter contents

The average organic carbon contents in the degraded vegetation area are the highest, with an average content of 17.62 mg/g, which is significantly higher than that in the other areas (Fig. 9). This probably occurs because the carbonated particles generated via vegetation withering increase the soil organic carbon contents by mixing with the soils (Cui et al. 2012; Zhao et al. 2016). In comparison, the organic matter contents in the Huangbaici coal fire area decreased with increasing soil temperature, because the heat effect of the coal fire digested the organic matter (Wang et al. 2020). We draw a nearly opposite conclusion: the average organic carbon contents in the high-temperature zone (area A) seem be higher than those in the surrounding area, and the mean average organic carbon contents in area A are significantly higher than those in area B (Fig. 9). The particles released through the fissures within the strata from the underground coal fires may increase the organic carbon contents (Wang et al. 2019). In addition, the landfilling with yellow sandy soil in area B affects the organic carbon contents because the sandy soil contains relatively low organic contents.

Limitations and future research directions

1) Breathing cycles are the common phenomena of certain coal fires. Engle et al. observed that the CO₂ vent

emissions in Wyoming coal fires significantly differ between two consecutive days, while the CO and H₂S showed no significant differences (Engle et al. 2012). Dindarloo et al. found that the CO concentration increased in the middle of the day when outside air temperature increased, and declined in the afternoon when the outside air cooled (Dindarloo et al. 2015). The temporal variability in diffuse gas emissions remains a research gap (Engle et al. 2013). Therefore, the temporal variability of in vent emissions and diffuse gas emissions in coal fire areas should be considered.

2) CO₂ generally stems from three sources in coal fire areas: native CO₂, CO₂ produced from coal combustion, and CO₂ produced from the oxidizing of native CH₄ (Ide and Orr 2011). Ide and Orr used ¹³C isotope signatures to determine the fractions of CO₂ emitted from coal combustion in coal seams (Ide and Orr 2011). Carras et al. found that the emission rate of greenhouse gases originating from low-temperature oxidation of coal waste is similar to the emission rates due to biological activity (Carras et al. 2009). In our study, CO₂ and CH₄ in areas A and B were qualitatively inferred to originate from coal combustion based on their relatively high concentrations and Pearson correlation analysis, as discussed in the “Analysis of the belowground gas concentration” section. A portion of CH₄ and CO₂ may originate from microbial activity in the degraded area. Quantitative analysis of the source is required in the research zones, which could determine contribution of the greenhouse gases emitted from coal combustion to the pollution of the local environment.

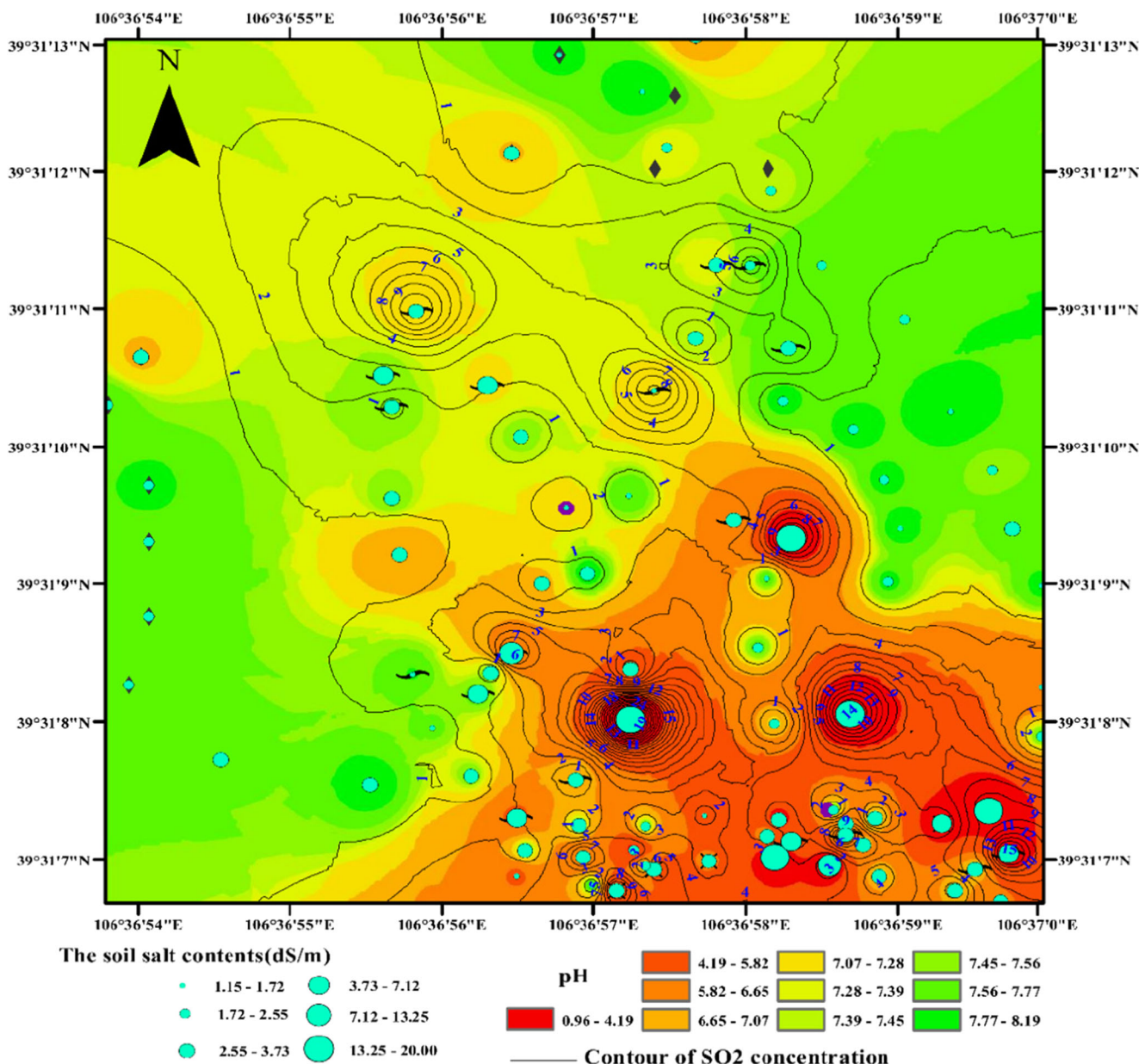


Fig. 7 The soil pH and total salt contents distribution in the research zone

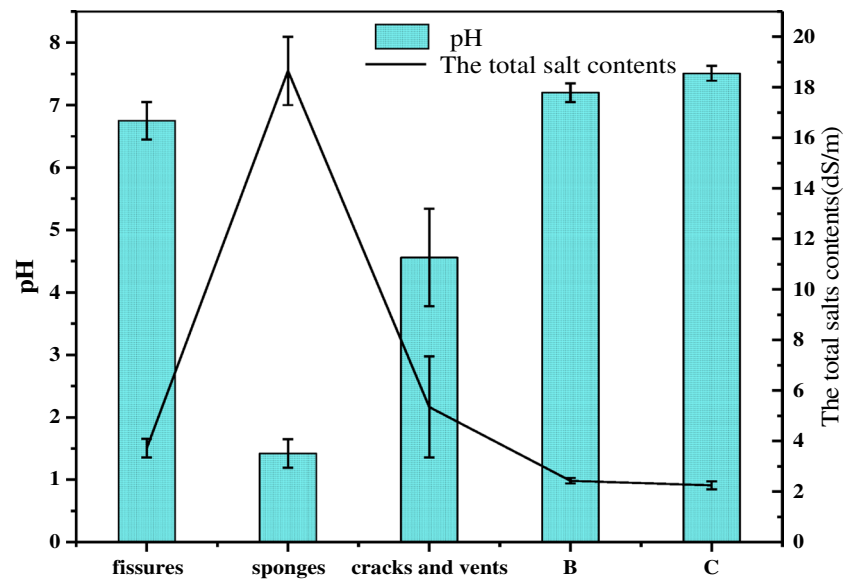
3) Soil chemical properties are sensitive to gas and heat intrusions as discussed in the “Limitations and future research directions” section, such as the soil pH and organic carbon. The mobility of trace metals and changes in microbial communities is reliably related to the soil pH and organic carbon (Rasheed et al. 2013). For example, the soil Hg and Cd contents were related to the organic matter (Wang et al. 2019), and Fe³⁺ concentration was relatively high near the vents (Querol et al. 2011). Tobin-Janzen found that the ribotype diversity of microbial populations decreased within individual boreholes with increasing temperature (Tobin-Janzen et al. 2005). Therefore, whether the change of soil biochemistry properties could be adopted a complementary index to monitor underground coal fires deserves further research.

Conclusion

Surveys were conducted in the Wuda coal fire area to investigate the impact of underground coal fires on the surface landform, soil gas emissions, and soil properties. Backfilling of sandy soil imposes certain effect on gas emissions and soil properties. These observations lead to the following conclusions:

- 1) Little vegetation occurs in the area seriously affected by underground coal fires, such as in area A and area B. Fissures, cracks and vents, and the sponges are the main fire-induced landforms in the research zone.

Fig. 8 pH and total salt contents comparison of the research zone

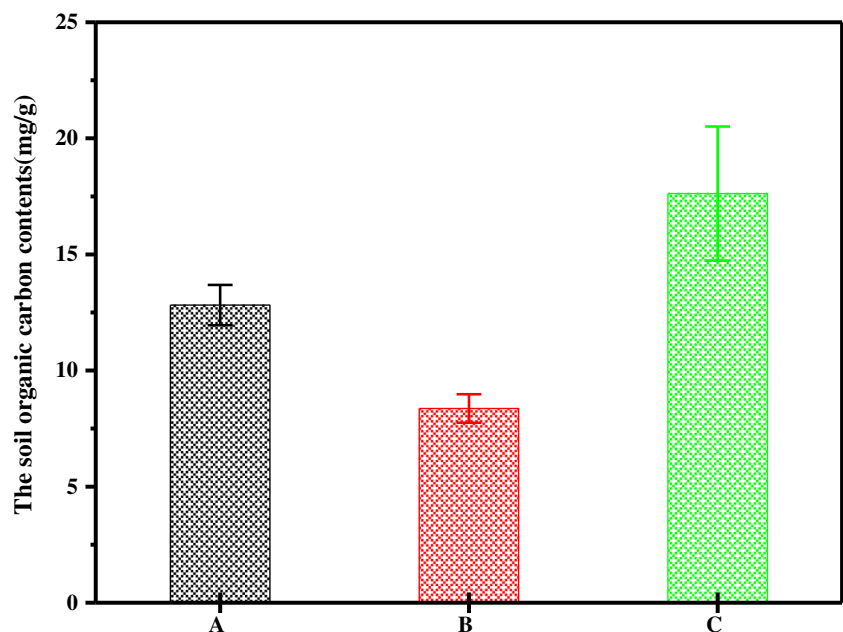


2) A comparison of the components and concentrations of gases is performed among area A, area B, and the degraded vegetation area. The CO_2 and CO concentrations peak at 11 vol% and 6008 ppm, respectively, in area A, far exceeding OSHA safety limits. In area B, the CO_2 and CO concentrations are relatively low, with average concentration of 9.84 vol% and 3530 ppm, respectively. SO_2 , H_2S , C_2H_6 , and C_2H_4 highly concentrate in area A, ranging from 0.72 to 26.4, 2 to 100, 6 to 128, and 2 to 74 ppm, respectively. The soil CO_2 concentrations are correlated with CH_4 but seem to be unrelated to CO. Low soil O_2 concentrations damage the healthy root environment for soil O_2 is displaced by CO_2 . CO and CH_4 are detected near the ground surface, while the other gases are below

the detection limits. Backfill of soil mitigates the emission of SO_2 , H_2S , C_2H_2 , and C_2H_6 , but does not seem to reduce emissions of the greenhouse gases in the research zone. The near-surface gas concentration mainly originates from the obvious openings. Although coal-fire gas emissions are diluted by air, the maximum of near surface CO concentration exceeds the OSHA 8-h exposure limit, which is a hazard to geologists at the site.

3) Thermal surface and soil moisture anomalies are mainly dominated by obvious openings. There seems no relationship between the surface temperature and gas concentration due to solar heating. The sponges exhibit the lowest soil pH (0.95–1.99), followed by the vents and cracks. A negative correlation is found between the soil pH and the

Fig. 9 Organic carbon contents comparison of the investigated area



total salt contents in area A ($r=0.859$, $p<0.01$). Hydrolysis of Al and Fe sulfates originating from soil salts accounts for the relatively low pH values. The particles released through the fissures may increase the organic carbon contents in area A, while the carbonated particles stemming from vegetation withering cause an increase in the organic carbon contents in the degraded vegetation area. Compared to the area A, the soil in area B attain relatively high soil pH values and relatively low organic carbon contents, which suggests that the soil cover helps improve the quality of the soil environment.

Funding This work was supported by National Natural Science Foundation of China (no. 51874313) and National Key R&D Program of China (no. 2018YFC0808101).

Declarations

Conflict of interest The authors declare that they have no competing interests.

References

- Carras JN, Day SJ, Saghabi A, Williams DJ (2009) Greenhouse gas emissions from low-temperature oxidation and spontaneous combustion at open-cut coal mines in Australia. *Int J Coal Geol* 78:161–168. <https://doi.org/10.1016/j.coal.2008.12.001>
- Cui XY, Hao JM, Zhao SS, Sang Y, Wang HQ, Di XY (2012) Temporal and spacial changes of total soil organic carbon content as affected by an experimental forest fire in the Greater Xing's a mountain. *J Soil Water Conserv* 26:195–200
- Dias CL, Oliveira MLS, Hower JC, Taffarel SR, Kautzmann RM, Silva LFO (2014) Nanominerals and ultrafine particles from coal fires from Santa Catarina, South Brazil. *Int J Coal Geol* 122:50–60. <https://doi.org/10.1016/j.coal.2013.12.011>
- Dindarloo SR, Hood MM, Bagherieh A, Hower JC (2015) A statistical assessment of carbon monoxide emissions from the Truman Shepherd coal fire, Floyd County, Kentucky. *Int J Coal Geol* 144–145:88–97. <https://doi.org/10.1016/j.coal.2015.03.012>
- Engle MA, Radke LF, Heffern EL, O'keefe JMK, Hower JC, Smeltzer CD et al (2012) Gas emissions, minerals, and tars associated with three coal fires, Powder River Basin, USA. *Sci Total Environ* 420:146–159. <https://doi.org/10.1016/j.scitotenv.2012.01.037>
- Engle MA, Olea RA, O'Keefe JMK, Hower JC, Geboy NJ (2013) Direct estimation of diffuse gaseous emissions from coal fires: current methods and future directions. *Int J Coal Geol* 112:164–172. <https://doi.org/10.1016/j.coal.2012.10.005>
- Garrison T, Hower JC, Fryar AE, D'Angelo E (2016) Water and soil quality at two eastern-Kentucky (USA) coal fires. *Environ Earth Sci* 75:574. <https://doi.org/10.1007/s12665-016-5380-4>
- Garrison T, O'Keefe JMK, Henke KR, Copley GC, Blake DR, Hower JC (2017) Gaseous emissions from the Lotts Creek coal mine fire: Perry County, Kentucky. *Int J Coal Geol* 180:57–66. <https://doi.org/10.1016/j.coal.2017.06.009>
- Gürdal G, Hoşgörmez H, Özcan D, Li X, Liu H, Song W (2015) The properties of Çan Basin coals (Çanakkale—Turkey): spontaneous combustion and combustion by-products. *Int J Coal Geol* 138:1–15. <https://doi.org/10.1016/j.coal.2014.12.004>
- Hong XP, Liang HD, Chen Y, Liu YH, Shi YY (2018) Distribution of fluorine in the surface dust of Wuda coal base, Inner Mongolia of Northern China. *J Geochem Explor* 188:390–397. <https://doi.org/10.1016/j.gexplo.2018.02.012>
- Hower JC, Henke K, O'Keefe JMK, Engle MA, Blake DR, Stracher GB (2009) The Tiptop coal-mine fire, Kentucky: preliminary investigation of the measurement of mercury and other hazardous gases from coal-fire gas vents. *Int J Coal Geol* 80:63–67. <https://doi.org/10.1016/j.coal.2009.08.005>
- Hower JC, O'Keefe JMK, Henke KR, Bagherieh A (2011) Time series analysis of CO concentrations from an Eastern Kentucky coal fire. *Int J Coal Geol* 88:227–231. <https://doi.org/10.1016/j.coal.2011.10.001>
- Hower JC, O'keefe JMK, Henke KR, Wagner NJ, Copley G, Blake DR et al (2013) Gaseous emissions and sublimates from the Truman Shepherd coal fire, Floyd County, Kentucky: a re-investigation following attempted mitigation of the fire. *Int J Coal Geol* 116–117:63–74. <https://doi.org/10.1016/j.coal.2013.06.007>
- Ide ST, Orr FM (2011) Comparison of methods to estimate the rate of CO₂ emissions and coal consumption from a coal fire near Durango, CO. *Int J Coal Geol* 86:95–107. <https://doi.org/10.1016/j.coal.2010.12.005>
- Jiang WG, Jia K, Chen Z, Deng Y, Rao PZ (2017) Using spatiotemporal remote sensing data to assess the status and effectiveness of the underground coal fire suppression efforts during 2000–2015 in Wuda, China. *J Clean Prod* 142:565–577. <https://doi.org/10.1016/j.jclepro.2016.03.082>
- Kuenzer C, Stracher GB (2012) Geomorphology of coal seam fires. *Geomorphology* 138:209–222. <https://doi.org/10.1016/j.geomorph.2011.09.004>
- Kuenzer C, Zhang JZ, Tetzlaff A, van Dijk P, Voigt S, Mehl H, Wagner W (2007) Uncontrolled coal fires and their environmental impacts: Investigating two arid mining regions in north-central China. *Appl Geogr* 27:42–62. <https://doi.org/10.1016/j.apgeog.2006.09.007>
- Li CH, Liang HD, Chen Y, Bai JW, Cui YK (2018) Distribution of surface soil mercury of Wuda old mining area, Inner Mongolia, China. *Hum Ecol Risk Assess Int J* 24:1421–1439. <https://doi.org/10.1080/10807039.2017.1413536>
- Liang YC (2018) Emission characteristics of typical pollutants of coal fire in Wuda, Inner Mongolia. Dissertation, China University of Mining and Technology (Beijing), Beijing
- Liang YC, Liang HD, Zhu SQ (2016) Mercury emission from spontaneously ignited coal gangue hill in Wuda coalfield, Inner Mongolia, China. *Fuel* 182:525–530. <https://doi.org/10.1016/j.fuel.2016.05.092>
- Liang Y, Zhu SQ, Liang HD (2018) Mercury enrichment in coal fire sponge in Wuda coalfield, Inner Mongolia of China. *Int J Coal Geol* 192:51–55. <https://doi.org/10.1016/j.coal.2018.03.006>
- O'keefe JM, Henke KR, Hower JC, Engle MA, Stracher GB, Stucker JD et al (2010) CO₂, CO, and Hg emissions from the Truman Shepherd and Ruth Mullins coal fires, eastern Kentucky, USA. *Sci Total Environ* 408:1628–1633. <https://doi.org/10.1016/j.scitotenv.2009.12.005>
- O'keefe JMK, Neace ER, Lemley EW, Hower JC, Henke KR, Copley G et al (2011) Old Smokey coal fire, Floyd County, Kentucky: estimates of gaseous emission rates. *Int J Coal Geol* 87:150–156. <https://doi.org/10.1016/j.coal.2011.06.005>
- O'keefe JMK, Neace ER, Hammond ML, Hower JC, Engle MA, East J et al (2018) Gas emissions, tars, and secondary minerals at the Ruth Mullins and Tiptop coal mine fires. *Int J Coal Geol* 195:304–316. <https://doi.org/10.1016/j.coal.2018.06.012>
- Oliveira MLS, Pinto D, Tutikian BF, da Boit K, Saikia BK, Silva LFO (2019) Pollution from uncontrolled coal fires: continuous gaseous emissions and nanoparticles from coal mines. *J Clean Prod* 215:1140–1148. <https://doi.org/10.1016/j.jclepro.2019.01.169>
- Patil RH, Colls JJ, Steven MD (2010) Effects of CO₂ gas as leaks from geological storage sites on agro-ecosystems. *Energy* 35:4587–4591. <https://doi.org/10.1016/j.energy.2010.01.023>

- Pone JDN, Hein KA, Stracher GB, Annegam HJ, Finkleman RB, Blake DR et al (2007) The spontaneous combustion of coal and its by-products in the Witbank and Sasolburg coalfields of South Africa. *Int J Coal Geol* 72:124–140. <https://doi.org/10.1016/j.coal.2007.01.001>
- Querol X, Izquierdo M, Monfort E, Alvarez E, Font O, Moreno T, Alastuey A, Zhuang X, Lu W, Wang Y (2008) Environmental characterization of burnt coal gangue banks at Yangquan, Shanxi Province, China. *Int J Coal Geol* 75:93–104. <https://doi.org/10.1016/j.coal.2008.04.003>
- Querol X, Zhuang X, Font O, Izquierdo M, Alastuey A, Castro I et al (2011) Influence of soil cover on reducing the environmental impact of spontaneous coal combustion in coal waste gobs: a review and new experimental data. *Int J Coal Geol* 85:2–22. <https://doi.org/10.1016/j.coal.2010.09.002>
- Rasheed MA, Lakshmi M, Rao PLS, Kalpana MS, Dayal AM, Patil DJ (2013) Geochemical evidences of trace metal anomalies for finding hydrocarbon microseepage in the petroliferous regions of the Tatipaka and Pasarlapudi areas of Krishna Godavari Basin, India. *Pet Sci* 10:19–29. <https://doi.org/10.1007/s12182-013-0245-x>
- Shan B, Wang G, Cao F, Wu D, Liang WX, Sun RY (2019) Mercury emission from underground coal fires in the mining goaf of the Wuda Coalfield, China. *Ecotoxicol Environ Saf* 182:109409. <https://doi.org/10.1016/j.ecoenv.2019.109409>
- Song ZY, Kuenzer C (2014) Coal fires in China over the last decade: a comprehensive review. *Int J Coal Geol* 133:72–99. <https://doi.org/10.1016/j.coal.2014.09.004>
- Song ZY, Kuenzer C (2017) Spectral reflectance (400–2500 nm) properties of coals, adjacent sediments, metamorphic and pyrometamorphic rocks in coal-fire areas: a case study of Wuda coalfield and its surrounding areas, northern China. *Int J Coal Geol* 171:142–152. <https://doi.org/10.1016/j.coal.2017.01.008>
- Song ZY, Kuenzer C, Zhu HQ, Zhang Z, Jia YR, Sun YL, Zhang JZ (2015) Analysis of coal fire dynamics in the Wuda syncline impacted by fire-fighting activities based on in-situ observations and Landsat-8 remote sensing data. *Int J Coal Geol* 141–142:91–102. <https://doi.org/10.1016/j.coal.2015.03.008>
- Song ZY, Wu DJ, Jiang JC, Pan XH (2019) Thermo-solutal buoyancy driven air flow through thermally decomposed thin porous media in a U-shaped channel: towards understanding persistent underground coal fires. *Appl Therm Eng* 159. <https://doi.org/10.1016/j.applthermaleng.2019.113948>
- Song ZY, Huang XY, Jiang JC, Pan XH (2020) A laboratory approach to CO₂ and CO emission factors from underground coal fires. *Int J Coal Geol* 219. <https://doi.org/10.1016/j.coal.2019.103382>
- Tobin-Janzen T, Shade A, Marshall L, Torres K, Beblo C, Janzen C et al (2005) Nitrogen changes and domain bacteria ribotype diversity in soils overlying the Centralia, Pennsylvania underground coal mine fire. *Soil Sci* 170:191–201. <https://doi.org/10.1097/00010694-200503000-00005>
- Wang YM, Li XQ, Wang WZ, Guo ZX (2017) Experimental and in-situ estimation on hydrogen and methane emission from spontaneous gasification in coal fire. *Int J Hydrog Energy* 42:18728–18733. <https://doi.org/10.1016/j.ijhydene.2017.04.192>
- Wang G, Cao F, Shan B, Meng M, Wang W, Sun RY (2019) Sources and assessment of mercury and other heavy metal contamination in soils surrounding the Wuda Underground Coal Fire Area, Inner Mongolia, China. *Bull Environ Contam Toxicol* 103:828–833. <https://doi.org/10.1007/s00128-019-02734-7>
- Wang HY, Zhang JP, Zhang L, Wang JL, Xu ZH (2020) Gas emission and soil chemical properties associated with underground coal fires, Wuda Coalfield, Inner Mongolia, China. *Nat Resour Res* 29:3973–3985. <https://doi.org/10.1007/s11053-020-09696-2>
- Zeng Q, Dong J, Zhao L (2018) Investigation of the potential risk of coal fire to local environment: a case study of Daquanhu coal fire, Xinjiang region, China. *Sci Total Environ* 640–641:1478–1488. <https://doi.org/10.1016/j.scitotenv.2018.05.135>
- Zhang T, Xu J, Zeng J, Lou K (2013) Diversity of prokaryotes associated with soils around coal-fire gas vents in MaNasi county of Xinjiang, China. *Antonie Van Leeuwenhoek* 103:23–36. <https://doi.org/10.1007/s10482-012-9782-3>
- Zhao ZX, Li ZC, Zhou JG, Cheng CF, Zhao RY, Sun JJ (2016) Effect of fire on soil organic carbon of natural *Pinus massoniana* forest in north subtropical area of China. *Chin J Ecol* 35:135–140